Ozone Depletion from Nearby Supernovae

Neil Gehrels

e-mail: gehrels@lheapop.gsfc.nasa.gov

NASA/GSFC/Laboratory for High Energy Astrophysics, Code 661, Greenbelt, MD 20771

Claude M. Laird

e-mail: claird@ku.edu

Department of Physics and Astronomy, University of Kansas, Lawrence, KS 66045

Charles H. Jackman

e-mail: jackman@assess.gsfc.nasa.gov

NASA/GSFC/Laboratory for Atmospheres, Code 916, Greenbelt, MD 20771

John K. Cannizzo[1]

e-mail: cannizzo@stars.gsfc.nasa.gov

NASA/GSFC/Laboratory for High Energy Astrophysics, Code 661, Greenbelt, MD 20771

Barbara J. Mattson[2]

e-mail: mattson@milkyway.gsfc.nasa.gov

NASA/GSFC/Laboratory for High Energy Astrophysics, Code 661, Greenbelt, MD 20771

Wan Chen

e-mail: Wan.W.Chen@mail.sprint.com

Sprint, ION Data Planning & Design, 12502 Sunrise Valley Dr., Reston, VA 20196

Received _____; accepted _____

[1]also University of Maryland Baltimore County

[2]also L3 Com Analytics Corp.

ABSTRACT

Estimates made in the 1970's indicated that a supernova occurring within tens of parsecs of Earth could have significant effects on the ozone layer. Since that time improved tools for detailed modeling of atmospheric chemistry have been developed to calculate ozone depletion, and advances have been made also in theoretical modeling of supernovae and of the resultant gamma ray spectra. In addition, one now has better knowledge of the occurrence rate of supernovae in the galaxy, and of the spatial distribution of progenitors to core-collapse supernovae. We report here the results of two-dimensional atmospheric model calculations that take as input the spectral energy distribution of a supernova, adopting various distances from Earth and various latitude impact angles. In separate simulations we calculate the ozone depletion due to both gamma rays and cosmic rays. We find that for the combined ozone depletion from these effects roughly to double the "biologically active" UV flux received at the surface of the Earth, the supernova must occur at $\lesssim 8$ pc.

Subject headings: molecular processes; Earth; stars: supernovae: general; supernovae: SN1978A; ISM: cosmic rays

1. Introduction

Ruderman (1974) suggested and was the first to study the reduction of stratospheric O_3 due to enhanced levels of nitrogen oxides caused by incident radiation from a supernova (SN). With rough calculations he found that a nearby (< 17 pc) SN would cause a reduction of O_3 by $\sim 80\%$ for > 2 yr from the gamma radiation, and a $40 - 90\%$ reduction in O_3 lasting hundreds of years from cosmic rays (Ruderman 1974, Laster 1968). Reid et al. (1978) reached similar conclusions, while Whitten et al. (1976) found a much smaller effect. Schramm & Ellis (1996) present a study similar to Ruderman's in which simple analytical scalings were utilized. Crutzen & Brühl (1996) also examine the problem using a time dependent two-dimensional (2D) model, considering only the enhanced gamma ray flux. Except for Crutzen & Brühl, these studies used simple theoretical models for the SN energy and had, at best, one-dimensional (1D) photochemistry models. Advances in computing power and atmospheric models now make a more detailed analysis possible. Also, SN1987A observations and recent state-of-the-art calculations provide an estimate for the total gamma ray input from a core-collapse SN.

2. Model

We model the effects of a core-collapse SN on the Earth's ozone by inputting the expected cosmic and gamma irradiation into an atmospheric model. We consider: (1) the relatively short-lived (~ 100 d) gamma rays from the initial blast, and (2) the longer lived (~ 20 y) cosmic rays accelerated in the SN blast wave. We examine the effects of SN distance and impact angle latitude, and determine the ozone depletion averaged latitudinally and globally. We use the NASA/Goddard Space Flight Center (GSFC) two-dimensional photochemical transport model (Jackman et al. 1990, 1996) after modifications by Vitt &

Jackman (1996) to incorporate energy deposition by solar proton events (SPEs) following Armstrong et al. (1989) and galactic cosmic rays (GCRs) from Nicolet (1975). The GSFC model is zonally averaged, has 18 latitude bands, and represents altitude with 58 evenly spaced logarithmic pressure levels (approximately 2 km vertical grid point separation) from the ground up to 116 km, and uses a time step of 1 d.

The observed gamma ray photon spectrum for SN1987A is

$$\frac{dN}{dE} = 1.7 \times 10^{-3} \left(\frac{E}{1 \text{ MeV}}\right)^{-1.2} \text{ cm}^{-1} \text{ s}^{-1} \text{ MeV}^{-1} \quad (1)$$

(Gehrels et al. 1988) between 0.02 and 2 MeV, lasting 500 d at 55 kpc, for a total energy 9.0×10^{46} erg. For ease of modeling we set the incident monoenergetic gamma ray photon flux N_i^0 by binning this differential flux into 66 evenly spaced logarithmic intervals from 0.001 to 10 MeV, for a net energy input of 3.3×10^{47} erg. For a given distance $D_{\rm SN}$ we scale the empirically observed SN1987A spectrum by $(5.5 \times 10^4/D_{\rm SN})^2$, with $D_{\rm SN}$ in pc. In addition, in our final analysis we rescale our results to a total gamma ray energy of 1.8×10^{47} erg because of the following: SN1987A was unusual in that its progenitor was a blue supergiant rather than the more typical red supergiant. A recent three-dimensional (3D) smooth particle hydrodynamics (SPH) calculation[3] of a SN with a $15 M_\odot$ red supergiant progenitor gives $\sim [1.8 \pm 0.7] \times 10^{47}$ erg for models which are initially spherically symmetric. In this model, the gamma ray luminosity peaks at $t \sim 340$ d and is within a factor of 10 of

[3]Aimee Hungerford kindly provided the results of her SN calculations in advance of publication. Her initial model, s15s7b from Weaver & Woosley (1993), was taken 100 s after bounce and mapped into a 3D SPH code. To calculate the gamma ray spectra and total energies, she mapped time slices from the SN calculation into a 3D Monte Carlo gamma ray transport code.

the peak for $\sim$ 500 d. Since the energies of the gamma ray photons are so much greater than those involved in the atmospheric chemistry reactions, the total input energy is more relevant than the detailed SN spectrum and we therefore have done all scalings using integrated energy inputs.

Treating the energy bins as monoenergetic beams of geometric mean energy $< E_i >$ and integrating over a range of energies (from $i = 1$ to 66), the incident photon flux is given by

$$N_i^0 = 8.5 \times 10^{-3} \left[E_i^{-0.2} - E_{i+1}^{-0.2} \right] \text{ cm}^{-2} \text{ s}^{-1} \tag{2}$$

where the total incident energy flux in the monoenergetic beam at the top of the atmosphere is $F_i^0 = N_i^0 < E_i >$. We attenuate the gamma ray photon flux with altitude via an exponential decay law, with the frequency-dependent absorption coefficient taken from a look-up table (Plechaty et al. 1981). The beam is propagated vertically through a standard atmosphere, which is adjusted later in the photochemistry model for the appropriate latitude and time of year. The photon flux remaining in a monoenergetic beam is given by $N_{i,j} = N_i^0 e^{-\mu_i x_j}$, where x_j is the column density (in g cm^{-2}) measured from the top of the atmosphere and μ_i is the mass attenuation or absorption coefficient for the ith energy bin (i.e., associated with energy $< E_i >$). The photon flux, $\Delta N_{i,j}$ (in photons cm^{-2} s^{-1}), deposited in the jth layer with energy $< E_i >$, is the difference between $N_{i,j-1}$ and $N_{i,j}$. The energy flux deposited in the jth layer by photons of energy $< E_i >$ is $F_{i,j} = \Delta N_{i,j} < E_i >$ (in MeV cm^{-2} s^{-1}). The total ionization rate is the sum over all energies

$$q_{\text{tot, } j} = \frac{1}{35 \text{ eV}} \sum_{i=1}^{66} \frac{F_{i,j}}{\Delta Z_j}, \tag{3}$$

where 35 eV is the energy required to produce an ion pair (Porter et al. 1976) and ΔZ_j is the thickness of the jth slab. The energy deposition versus altitude calculated in this way

is not dramatically different from that obtained using a detailed radiative transfer model.[4]

We estimate the SN cosmic ray inputs from the galactic cosmic ray (GCR) ionization rate profiles at various latitudes and solar cycle phase (Vitt & Jackman 1996, Nicolet 1975). The mean rate of nitrogen atom (N) production at different altitudes and latitudes is computed by multiplying the empirically computed rate of ionization (from Nicolet 1975) by 1.25 (Jackman et al. 1990). The N production enhances nitrogen oxide amounts as well as total odd nitrogen, NO_y (e.g., N, NO, NO_2, NO_3, N_2O_5, HNO_3, HO_2NO_2, $ClONO_2$, and $BrONO_2$). The local GCR energy density ~ 1 eV cm^{-3} is dominated by protons with a peak at ~ 0.5 GeV (Webber 1998), implying a flux ~ 7 cm^{-2} s^{-1}. Each incident cosmic ray produces $\sim 10^7$ ionizing secondary particles. The GCR ionization rate inputs (from Nicolet 1975) were multiplied by 100 to simulate the charged particle flux from a SN at 10 pc, and scaled by (10 pc/$D_{\rm SN}$)^2 for other distances. For $D_{\rm SN} = 10$ pc, the locally observed GCR flux ~ 0.05 erg cm^{-2} s^{-1} becomes ~ 5 erg cm^{-2} s^{-1}, yielding a total energy $\sim 4 \times 10^{49}$ erg over a 20 y run. The corresponding fluence is $\sim 3 \times 10^9$ erg cm^{-2}.

The vertical ionization rate profiles are then mapped onto a 2D circular grid, representing a zonally averaged spherical Earth. First a series of ionization rate profiles as functions of atmospheric slab number and latitude are calculated for a flat Earth for incidence angles of 5°, 15°,..., 85° from the zenith, corresponding to 10° wide latitude bands centered on 85°, 75°,..., 5°, respectively, for the illuminated hemisphere. These profiles are interpolated to produce vertical average ionization profiles as functions of altitude and latitude. The zenith frame daily ionization profiles are mapped into 360 intervals of 1°

---

[4]We thank David Smith, John Scalo, and Craig Wheeler for kindly sharing results from their Monte Carlo atmospheric radiative transfer calculation. The robustness of adopting simple energy-dependent attenuation coefficients in terms of the energy deposition versus altitude was first shown by Chapman (1931).

longitude and 18 intervals of 10° latitude. Zonally averaged daily ionization rate profiles are produced by averaging over all longitudes for each 10° latitude band, and then input into the GSFC 2D model.

Three types of calculations of 20 y duration were carried out: (1) a "base" simulation with no cosmic or gamma rays, (2) "perturbed" simulations with enhanced cosmic ray levels, and (3) "perturbed" simulations with enhanced gamma rays. The "perturbed" simulations were compared to the "base" simulation to assess the atmospheric changes. For the cosmic ray trials, the charged particle fluxes are held constant for 20 y, and the results are then checked to ensure a steady state is achieved. For the gamma ray trials, the irradiation is activated on day 60 (March 1) and maintained at a constant level for 300 d (the SN duration), after which it is attenuated abruptly while the model is run for another 19 y, allowing the perturbed atmosphere time to relax to pre-SN conditions.

3. Results

Five gamma-ray simulations were performed for SN impact angle latitude (i.e., latitude for which the SN is at zenith) $i_{SN} = -90°$, $-45°$, $0°$, $+45°$, and $+90°$, taking $D_{SN} = 10$ pc. Three more simulations were carried out for $i_{SN} = 0°$ and $D_{SN} = 20$, 50, and 100 pc. We find that after 300 d of simulated gamma radiation input, the calculated changes in NO_y and O_3 column density depend significantly on i_{SN}. The largest increases in NO_y for $D_{SN} = 10$ pc are for $i_{SN} = \pm 90°$, and exceed 1800% over the poles. The smallest increases occur for $i_{SN} = 0°$, where the maximum increase is $< 900\%$ by the end of the run. Ozone depletion accompanying the increase in NO_y is greatest for $i_{SN} = \pm 90°$, with the zone of maximum decrease ($\sim 60\%$) at 60-70° S latitude for $i_{SN} = -90°$. The smallest decrease occurs for $i_{SN} = 0°$, with the region of maximum decrease (about 40%) at 60-90° S latitude (Figures 1 and 2). The maximum annual global average decrease for $D_{SN} = 10$ pc (Figure

3) is 27% in Year 2 for $i_{SN} = 0°$; the minimum is 18% for $i_{SN} = -90°$. Simulations for 10, 20, 50, and 100 pc show a $\sim D_{SN}^{-n}$ trend in ozone depletion, where $\sim 1.3 < n <\sim 1.9$ (Figure 4). In all cases, the global average ozone depletion from enhanced gamma rays decreases to a few percent by the sixth or seventh year.

Figure 4 shows an increasing deviation from a D_{SN}^{-2} law for the ozone depletion as D_{SN} decreases. In other words, although the fluence or net energy input from gamma rays varies (by assumption) as D_{SN}^{-2}, the ozone depletion begins to saturate for small D_{SN}. Three processes lead to this deviation: 1) The reaction of N with NO limits the production of NO_y in the limit where the NO_y concentration becomes too high; in effect NO_y begins to become self-destructive (Crutzen & Brühl 1996). 2) Ozone can be produced (rather than destroyed) by enhancements of NO_y in the troposphere and in the lowest part of the tropical stratosphere (Crutzen & Brühl 1996), a consideration which becomes increasingly important for higher rates of energy deposition. 3) Finally, the enhanced NO_y begins to interfere with other families (e.g., chlorine-, bromine-, and hydrogen-containing constituents) that destroy ozone, thus reducing the resultant ozone destruction from those families (e.g., this mechanism for production of NO_y due to extremely large solar proton events was discussed in Jackman et al. 2000).

For cosmic ray simulations, we find that after achieving the perturbed steady state, NO_y column densities increase at all latitudes and for all times of the year. For $D_{SN} = 10$ pc, the largest increases in column NO_y (650%) occur over the North Pole in late summer, while the smallest increases (200%) occur over the South Pole in winter, with an average global increase of about 350%. Corresponding column O_3 levels decrease globally and in all seasons by as much as 40% over the North Pole, in late summer and by as little as 5% over the equator during May-August for an average global decrease of 22%. Our global ozone reductions are less than those of Ruderman (1974) and Reid et al. (1978), but consistent

with Whitten et al. (1976).

4. Discussion

In order to quantify the impact on life of different levels of ozone depletion, we use the results of Madronich et al. (1998). From their Table 1 and Figure 2, we take a factor of ~ 2 increase in the biologically active UV flux to be a threshold for significant biological effects. This increase corresponds to an ozone depletion of $\sim 47\%$, given that the biologically active UV flux scales roughly as the reciprocal of the ozone column (Madronich et al. 1998).[5] There will probably be an interference between the increases in NO_y caused by the gamma rays and cosmic rays, therefore a summation of the separately computed ozone depletions from the two effects will result in a maximum estimate of the total SN influence. Summing our gamma ray and cosmic ray depletions for $D_{\rm SN} = 10$ pc, and taking into account that our adopted energy is larger than that found in the latest SN study mentioned earlier, we obtain a fiducial "critical distance" to significantly disrupt ozone of $D_{\rm crit} \simeq 8$ pc for a SN with a total gamma ray energy $\sim 1.8 \times 10^{47}$ erg.

The impulsive addition of energy into the atmosphere by other types of catastrophes

[5]Although the exponential, or Beer-Lambert model, for attenuation is a good approximation at a given wavelength, it is not appropriate for biological effects at the Earth's surface. The biological spectral sensitivity depends on the integrated UV flux between about 290 nm and 330 nm. One can show analytically that the biologically active UV flux varies roughly as the reciprocal of the ozone column given that (i) the ozone absorption cross section decreases exponentially with wavelength in this spectral region (290–330 nm), and (ii) the biological action spectrum decreases exponentially with wavelength over this same spectral region (Madronich et al. 1998).

may also lead to the production of NO_y, therefore the accompanying destruction of ozone may not be unique to the SN scenario. A dilution factor of $\sim 10^{-22}$ for the cross section of the Earth as seen from 10 pc means that the SN gamma ray energy of 2×10^{47} erg translates to $\sim 2 \times 10^{25}$ erg intercepted by the Earth. An asteroid with mass $\sim 3 \times 10^{17}$ g and speed ~ 25 km s^{-1} such as the one responsible for the Cretaceous-Tertiary extinction (Alvarez et al. 1980) has $\sim 10^{30}$ erg of kinetic energy (KE), so that even if as little as $\sim 10^{-5}$ of the KE were channeled into atmospheric heating, it would rival the SN input. On the other hand, the creation of NO_y through a sudden event would probably be less long lasting: First, the transport of NO_y from the stratosphere to the troposphere would occur over a few years. Tropospheric NO_y exists mainly as HNO_3, and would be removed by precipitation. Second, a localized event in the atmosphere would probably not be communicated globally. For instance, if an asteroid generated NO_y along its trajectory through the atmosphere, it would not necessarily mix globally on a time scale short compared to its destruction time scale. A period of sustained energy input is required to maintain continuously high levels of NO_y if the depletion of ozone is to be effective.

For a nearby SN to disrupt life on Earth, there must be some finite probability that such an event has occurred within the past several hundred million years. For our galaxy the SN rate is ~ 1.5 per century (Cappellaro et al. 1999). Clark et al. (1977) estimate the Sun should pass within 10 pc of a SN during each spiral arm passage, implying a SN rate of ~ 10 Gyr^{-1}. Two key issues affecting the SN rate are (i) the vertical scale height $h_{\rm SN}$ over which supernovae (SNe) are distributed, and (ii) the displacement of the solar system from the galactic plane. The study of Clark et al., for example, ignores the vertical disk structure and concludes that every passage through a spiral arm results in a close-proximity SN. An opposing view is presented by van den Bergh (1994) who adopts $h_{\rm SN} = 300$ pc, thereby giving ~ 0.3 Gyr^{-1} for SNe within 10 pc. Maiz-Apellaniz (2001) utilizes a sample of O-B5 stars, precursors to core-collapse SNe, obtained from the *Hipparchos* catalog to determine

$h_{SN} = 34$ pc. He also finds the Sun to be ~ 24 pc above the galactic plane – a value that is fortuitously less than h_{SN}. The value $h_{SN} \simeq 30$ pc is a factor of ~ 10 less than that used by van den Bergh, and leads to a SN rate intermediate between van den Bergh and Clark et al., i.e., ~ 3 Gyr^{-1} for $D_{SN} < 10$ pc, or ~ 1.5 Gyr^{-1} for $D_{SN} < D_{crit} \simeq 8$ pc, where we used the fact that the rate varies as D_{SN}^3.

One potential caveat to this line of reasoning in which the assumed SN fluences vary as D_{SN}^{-2} is the possibility that the Earth may lie within a bubble of hot gas caused by recent SNe, so that when a new SN occurs the cosmic ray influence within the bubble may be more isotropic and therefore stronger. Benitez et al. (2002) make this argument concerning recent SNe in the Local Bubble and the Scorpius-Centaurus OB association which may have generated ~ 20 SNe in the last ~ 10 Myr. The cosmic ray flux $\phi_{CR} \lesssim 1.4 \times 10^7$ erg cm^{-2} y^{-1} quoted by Benitez et al. using the minimal distance for the Sco-Cen SNe $D_{SN} \gtrsim 40$ pc is actually about a factor of 10 less than we adopt in this work for $D_{SN} = 10$ pc, leading us to believe the effect discussed by Benitez et al. may produce ozone depletions of only a few percent. Nevertheless the complications introduced by having the Earth be inside a hot bubble which may enhance the cosmic ray flux during an interval in which several successive SNe occur are interesting and worthy of more detailed studies.

5. Conclusion

In summary, we have calculated detailed atmospheric models to determine the extent of the reduction in ozone due to elevated levels of odd nitrogen induced from gamma rays and cosmic rays produced in a local SN. Our procedure is as follows: (i) We utilize a detailed 2D model for the Earth's atmosphere, incorporating the latest advances in photochemistry and transport. (ii) For the gamma ray spectrum we take as input the observed spectrum from SN1987A, scaling the total energy to the most recent value determined by workers

investigating core-collapse SNe with a red supergiant progenitor. (iii) For the cosmic ray spectrum we adopt scaled-up values of the empirically observed ionization rates in the atmosphere from galactic cosmic rays. (iv) To estimate the frequency of local SNe we utilize recent estimates of global SN rates for spiral galaxies and the results of a recent investigation into the vertical spatial extent of core-collapse SN progenitors. Our primary finding is that a core-collapse SN would need to be situated approximately 8 pc away to produce a combined ozone depletion from both gamma rays and cosmic rays of $\sim 47\%$, which would roughly double the globally-averaged, biologically active UV reaching the ground. The rate of core-collapse SNe occurring within 8 pc is ~ 1.5 Gyr^{-1}. As noted earlier, our calculated ozone depletion is significantly less than that found by Ruderman (1974), and consistent with Whitten et al. (1976). Given the ~ 0.5 Gyr time scale for multicellular life on Earth, this extinction mechanism appears to be less important than previously thought.

It is a pleasure to acknowledge stimulating conversations with Frank Asaro, Narciso Benitez, Adam Burrows, Enrico Cappellaro, Aimee Hungerford, Sasha Madronich, Frank McDonald, John Scalo, David Smith, Floyd Stecker, Sidney van den Bergh, William Webber, Craig Wheeler, and Stan Woosley.

REFERENCES

Alvarez, L. W., Alvarez, W., Asaro, F., & Michel, H. V. 1980, Science, 208, 1095

Armstrong, T. P., Laird, C. M., Venkatesan, D., Krishnaswamy, S., & Rosenberg, T. J. 1989, J. Geophys. Res., 94, 3543

Benitez, N., Maiz-Apellaniz, J., & Canelles, M. 2002, Phys. Rev. Lett., 88, 081101-1

Cappellaro, E., Evans, R., & Turatto, M. 1999, A&A, 351, 459

Chapman, S. 1931, Proc. Phys. Soc., 43, 26

Clark, D. H., McCrea, W. H., Stephenson, F. R. 1977, Nature, 265, 318

Crutzen, P. J., & Brühl, C. 1996, Proc. Natl. Acad. Sci. USA, 93, 1582

Ellis, J., & Schramm, D. N. 1995, Proc. Natl. Acad. Sci. USA, 92, 235

Gehrels, N., Leventhal, M., MacCallum, C. J., 1988, in Nuclear Spectroscopy of Astrophysical Sources, AIP Conf. 170, eds. N. Gehrels, G. Share (AIP, New York), 87

Jackman, C. H., Douglas, A. R., Rood, R. B., & McPeters, R. D. 1990, J. Geophys. Res., 95, 7417

Jackman, C. H., Fleming, E. L., Chandra, S., Considine, D. B., & Rosenfield, J. E. 1996, J. Geophys. Res., 101, 28753

Jackman, C. H., Fleming, E. L., & Vitt, F. M. 2000, J. Geophys. Res., 105, 11659

Laster, H. 1968, Science, 160, 1138

Madronich, S., McKenzie, R. L., Bjorn, L. O., Caldwell, M. M. 1998, J. Photochem. and Photobiol. B Biology, 46, 5

Maiz-Apellaniz, J. 2001, AJ, 121, 2737

Nicolet, M. 1975, Planet. Space Sci., 23, 637

Plechaty, E. F., Cullen, D. E., & Howerton, R. J. 1981, Tables and Graphs of Photon-Interaction Cross Sections From 0.1 keV to 100 MeV Derived From the LLL Evaluated Nuclear-Data Library Tables and Graphs of Photon-Interaction Cross (Lawrence Livermore Laboratory; Berkeley)

Porter, H. S., Jackman, C. H., & Green, A. E. S. 1976, J. Chem. Phys., 65, 154

Reid, G. C., McAffee, J. R., & Crutzen, P. J. 1978, Nature, 275, 489

Ruderman, M. A. 1974, Science, 184, 1079

van den Bergh, S. 1994, PASP, 106, 689

Vitt, F. M., & Jackman, C. H. 1996, J. Geophys. Res., 101, 6729

Weaver, T. A., & Woosley, S. E. 1993, Phys. Rep., 227, 65

Webber, W. R. 1998, ApJ, 506, 329

This manuscript was prepared with the AAS LaTeX macros v3.0.

FIGURE CAPTIONS

Figure 1. Contour plot of global average of ozone depletion during Year 2 from gamma irradiation, for $D_{SN} = 10$ pc and $i_{SN} = 0°$.

Figure 2. Contour plot of global average of ozone depletion during Year 20 due to the cosmic irradiation, assuming an enhancement of 100-fold in the empirically observed GCR ionization rate, and $i_{SN} = 0°$.

Figure 3. Peak annual average reduction in global ozone from gamma irradiation for $D_{SN} = 10$ pc as a function of i_{SN} (average over Year 2).

Figure 4. Annual average reduction in global ozone from gamma irradiation from a SN as a function of D_{SN}, assuming $i_{SN} = 0°$ (average over Year 2). The solid line indicates a dependency of D_{SN}^{-2}.

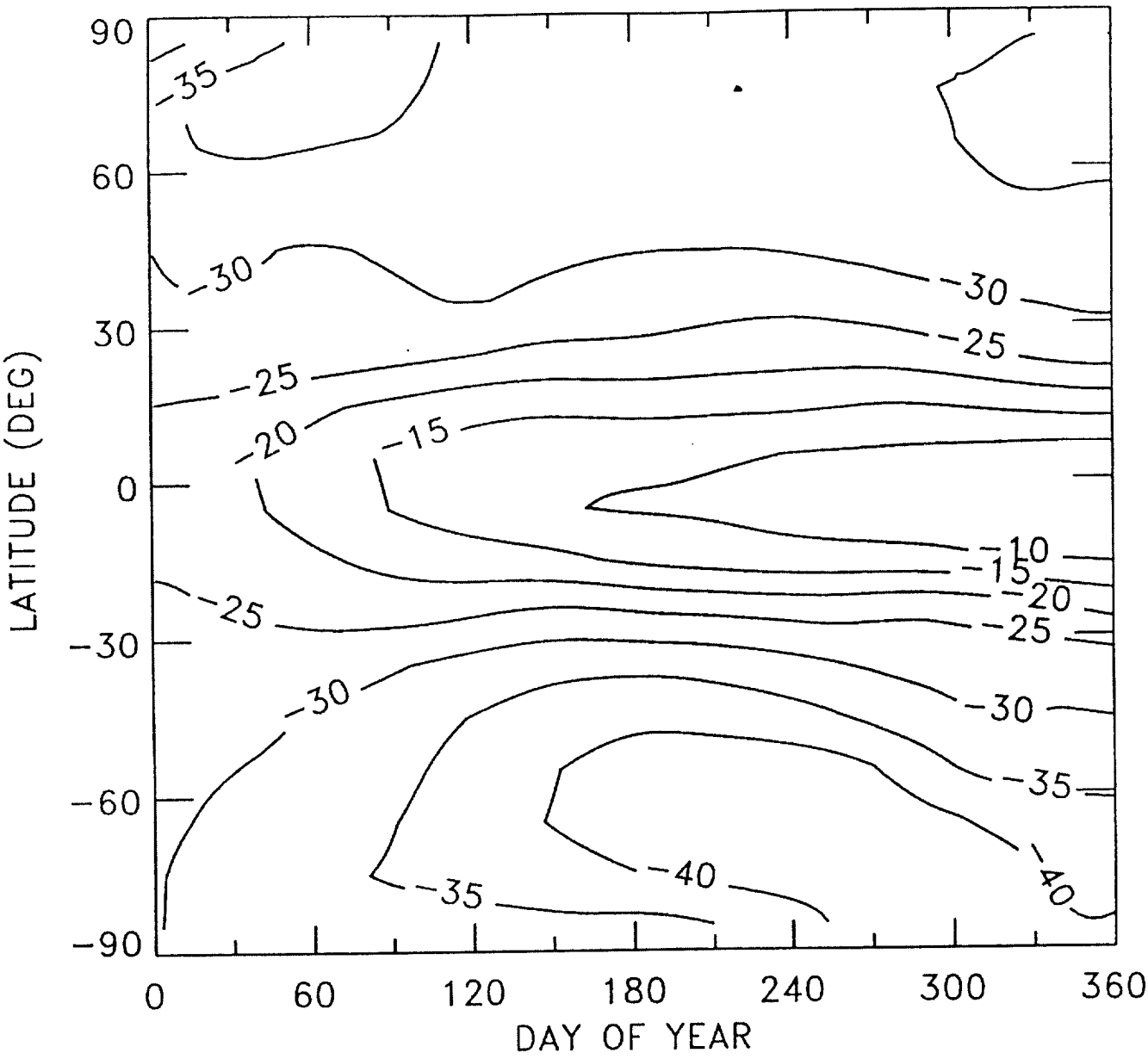
90
60
30
0
-30
-60
-90
LATITUDE (DEG)
0
60
120
180
240
300
360
DAY OF YEAR
-35
-30
-25
-20
-15
-10
-40

Fig. 1

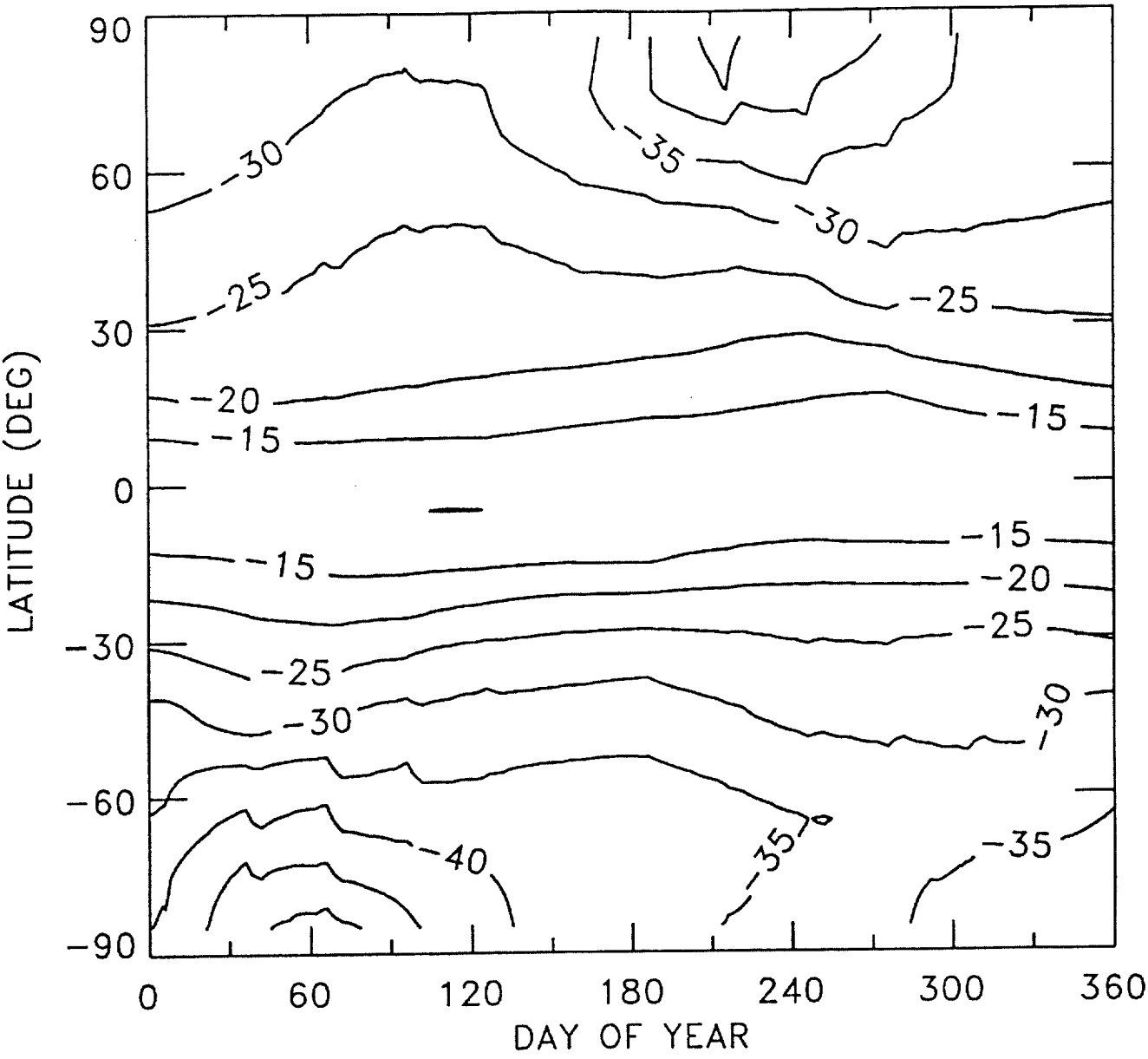
90
60
30
0
-30
-60
-90
LATITUDE (DEG)
0
60
120
180
240
300
360
DAY OF YEAR
-30
-35
-30
-25
-25
-20
-15
-15
-15
-15
-20
-25
-25
-30
-30
-40
-35
-35

fig. 2

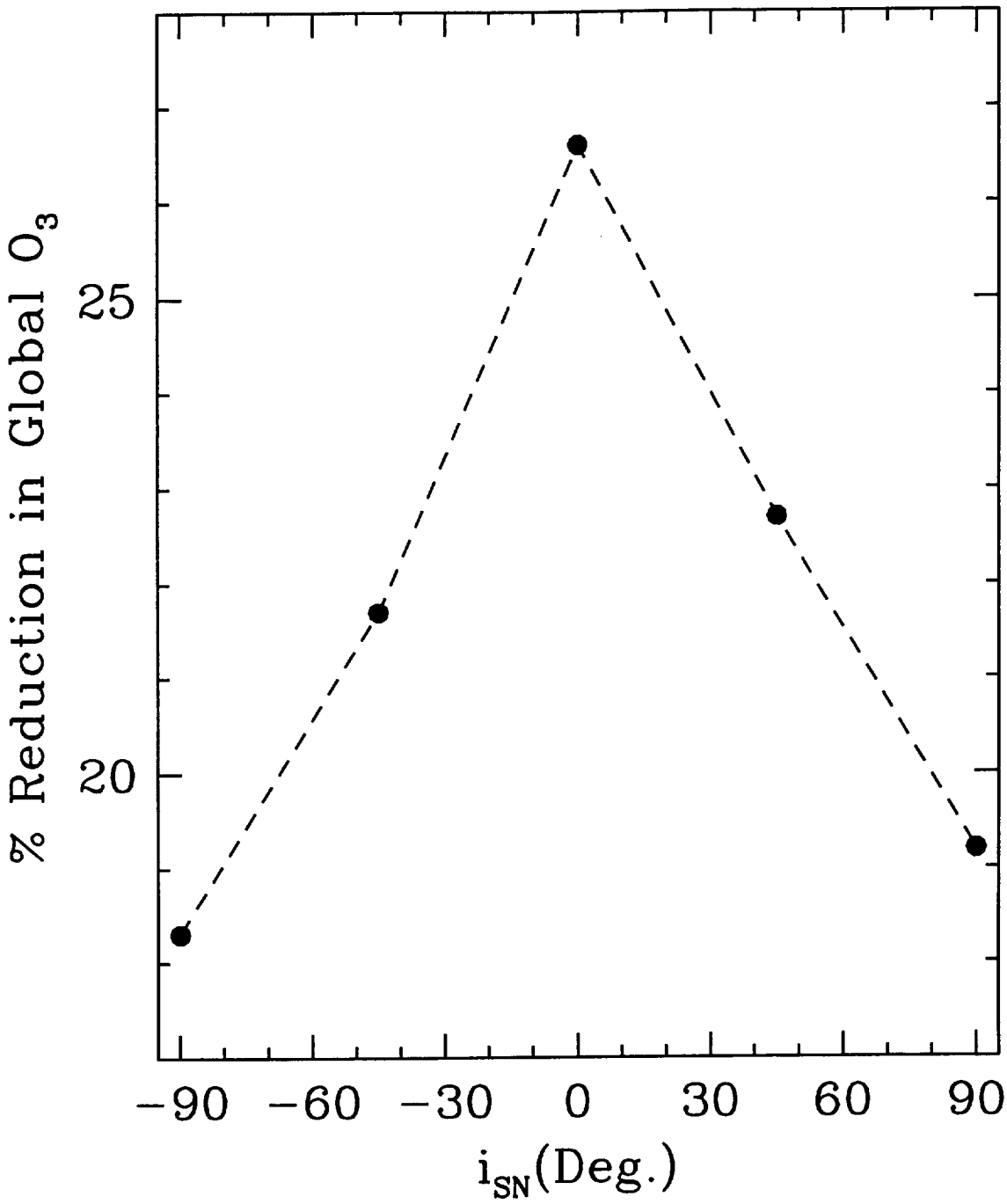

Fig. 3

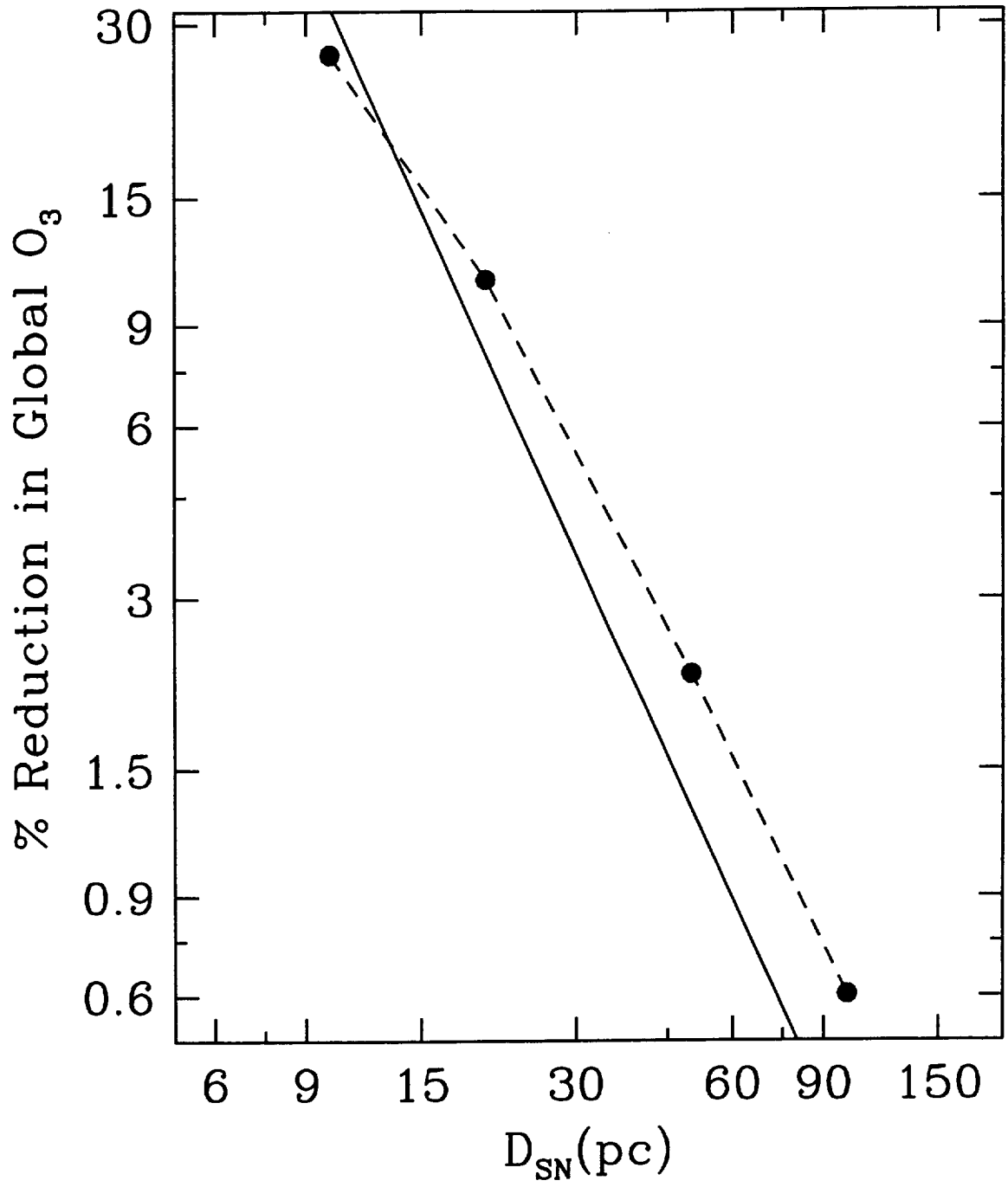
30
15
9
6
3
1.5
0.9
0.6
% Reduction in Global O_3
6
9
15
30
60
90
150
D_{SN}(pc)

Fig. 4